

## An insertion device for the soft X-ray photochemistry beamline at SPring-8

Takashi Tanaka,\* Xavier-Marie Maréchal, Toru Hara, Toshiya Tanabe and Hideo Kitamura

SPring-8, Kamigori-cho, Hyogo 678-12, Japan.

E-mail: ztanaka@spring8.or.jp

(Received 4 August 1997; accepted 15 October 1997)

A figure-8 undulator is an insertion device (ID) proposed at SPring-8 to reduce the heat-load problems encountered with ordinary linear undulators. This device is useful when the  $K$  value is high in order to obtain low-energy photons as the fundamental of the undulator radiation. It has therefore been adopted as the ID for the soft X-ray photochemistry beamline (BL27SU) at SPring-8 because linearly polarized photons between 100 and 2000 eV are necessary for the experiments on this beamline. The figure-8 undulator for BL27SU is now under construction and, in the first phase of operation, is expected to cover the energy range down to 500 eV. In the second and third phases, the lowest energy may be reduced to 170 and 100 eV, respectively.

**Keywords:** undulators; low heat loads.

### 1. Introduction

At the beamline for soft X-ray photochemistry (BL27SU) at SPring-8, a linearly polarized soft X-ray beam is necessary. However, the electron energy at SPring-8 is slightly too high to provide soft X-rays using an undulator, meaning that the periodic length should be long or the  $K$  value should be high. Long periodic length means the degradation of the number of periods; therefore, a high  $K$  value is necessary to obtain high brilliance. However, high  $K$  values cause an increase of higher harmonics in the case of a linear undulator, resulting in unreasonable heat loads (Kitamura, 1995).

A figure-8 undulator is an insertion device (ID) proposed to reduce the heat-load problems encountered with ordinary linear undulators (Tanaka & Kitamura, 1995). The radiation from a figure-8 undulator has the advantage that the on-axis power density is much lower than that from a linear undulator, while the photon flux density is almost the same. Therefore, a figure-8 undulator has been fitted as an ID for BL27SU.

### 2. Features of a figure-8 undulator

The features of a figure-8 undulator are described below to clarify why one has been adopted as an ID for BL27SU.

The trajectory in the figure-8 undulator is shown in Fig. 1. It looks like a figure 8 when projected on the transverse plane. In the upper part of the trajectory, the direction of rotation is left handed while that in the lower part is right handed. Because linear polarization is regarded as the superposition of right- and left-handed circular polarization, the total polarization obtained from the figure-8 trajectory may be linear. In addition, the on-axis

**Table 1**

Specifications of the figure-8 undulator for BL27SU at SPring-8.

Asterisks denote values that are expected to be achieved in future.

Permanent magnet	Nd-Fe-B
Remanent field	1.3 T
Periodic length	100 mm
Number of periods	44
Length of ID	4.4 m
Minimum gap	30 (20*) mm
Maximum gap	290 mm
Maximum vertical field	0.741 (1.031*) T
Maximum horizontal field	0.232 (0.261*) T
Maximum $K_y$ value	6.92 (9.63*)
Maximum $K_x$ value	4.23 (4.88*)
Available energy	170 (100*)–5.0 keV
Polarization	Horizontal and vertical
Type of device	Figure-8

power density is as low as that of a helical undulator because the figure-8 trajectory can be considered as the superposition of right- and left-handed helices.

Examples of spectra obtained from linear and figure-8 undulators are shown in Figs. 2(a) and 2(b), respectively. The electron energy is assumed to be 8 GeV, the average current 100 mA, the periodic length 10 cm and the number of periods 44. The  $K$  values are set at 4.72 (linear) and 3.34 ( $= K_x = K_y$ , figure-8). In this case the energy of the fundamental is 500 eV. In the case of a linear undulator, higher harmonics rather than the fundamental radiation greatly contribute to the spectrum, meaning that the on-axis power density is unreasonably high (98 kW mrad<sup>-2</sup>). On the other hand, higher harmonics above 10 keV have almost disappeared in the case of the figure-8 undulator and the on-axis power density is much lower than that of the linear undulator (1.4 kW mrad<sup>-2</sup>). Because the difference of the photon flux density at 500 eV is small, a figure-8 undulator has been adopted, instead of a linear undulator, as an ID to obtain linearly polarized soft X-rays at SPring-8.

Another spectral feature of the figure-8 undulator is that in addition to integer harmonics, half-odd-integer harmonics appear in the spectra. It is found from a simple calculation that integer harmonics have horizontal polarization, while half-odd-integer harmonics have vertical polarization.

### 3. Specifications

Table 1 shows the specifications of the figure-8 undulator for BL27SU at SPring-8. During the first phase of operation, the

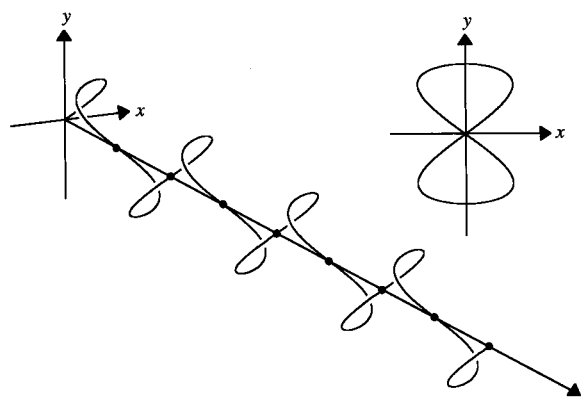


**Figure 1**  
Trajectory in the figure-8 undulator.

thickness of the vacuum chamber will be 28 mm; therefore, the minimum gap will be 30 mm including an alignment error. After the storage ring has made specific progress, the chamber will be exchanged for one with a thickness of 18 mm that will allow a minimum gap of 20 mm.

Although the lowest energy of the fundamental is 100 eV at a gap of 20 mm, it should be noted that 50 eV is also provided as the 0.5th harmonic.

#### 4. Operation phase

As described in the previous section, in the first phase the minimum gap is limited by the vacuum-chamber thickness to 30 mm; however, there is another limitation which determines the minimum gap in the first phase.

In the bending-magnet chamber located just behind the ID, there is a part called a 'slot', where the vertical aperture is narrow. Because the vertical divergence of radiation power from an ID is proportional to the strength of the horizontal field ( $K_x$ ), it is necessary to keep  $K_x$  lower than a specific value (the  $K_x$  limit) so that the radiation does not damage the wall of the slot.

Figs. 3(a)–3(c) show spatial distributions of the power density obtained from the figure-8 undulator for various gap values. The  $K$  values indicated in the figure caption are calculated in the case of the magnetic arrangement shown in Fig. 3. Cross-hatched areas show the slot of the bending-magnet chamber including an alignment error. If we assume that the maximum power density

allowed to hit the slot is  $0.15 \text{ kW mrad}^{-2}$ , equivalent to the one tenth of the power density from the bending magnet, the  $K_x$  limit is determined to be 3.29 [case (b)]. Therefore, the minimum gap in the first phase of operation is found to be 50 mm. In this case, the energy of the fundamental is 500 eV.

If the temperature increase of the slot due to the heat load is negligible or a solution to the heat-load problem is found (e.g. a cooling system), the gap can be reduced to 30 mm. This is the minimum gap in the second phase.

In the third phase, the vacuum chamber will be exchanged for one with a thickness of 18 mm and the minimum gap will be 20 mm.

Fig. 4 shows the gap dependence of the vertical and horizontal magnetic fields. Also shown is the energy of the fundamental. It is found that the lower limits of the available energy in the first, second and third phases are 500, 170 and 100 eV, respectively.

#### 5. Conclusions

The figure-8 undulator for BL27SU described in this paper has been delivered to the SPring-8 site and field measurements and corrections are now in progress. If there are no problems, it will be installed in the storage ring at the end of 1997.

It should be noted that the horizontal field,  $K_x$ , of the figure-8 undulator pushes away higher harmonics off-axis and suppresses the on-axis power density. Simultaneously, it decreases the intensity of the fundamental radiation; there may therefore be an

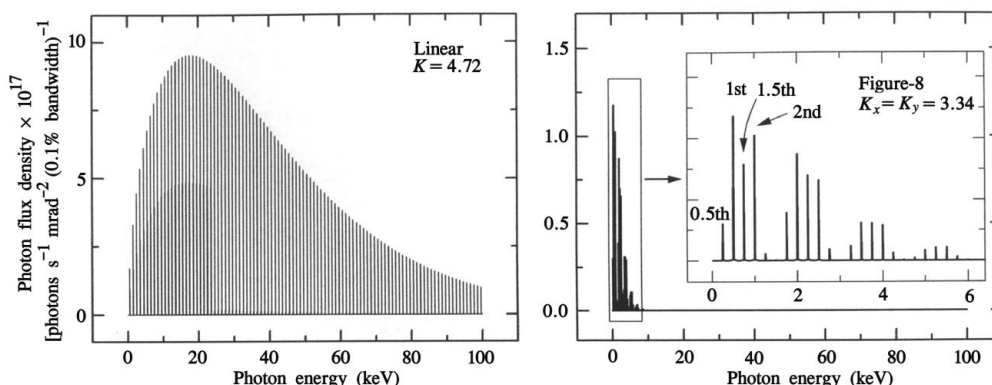


Figure 2

Examples of spectra obtained from (a) linear and (b) figure-8 undulators. In (b), the detail of the spectrum up to 6 keV is also shown.

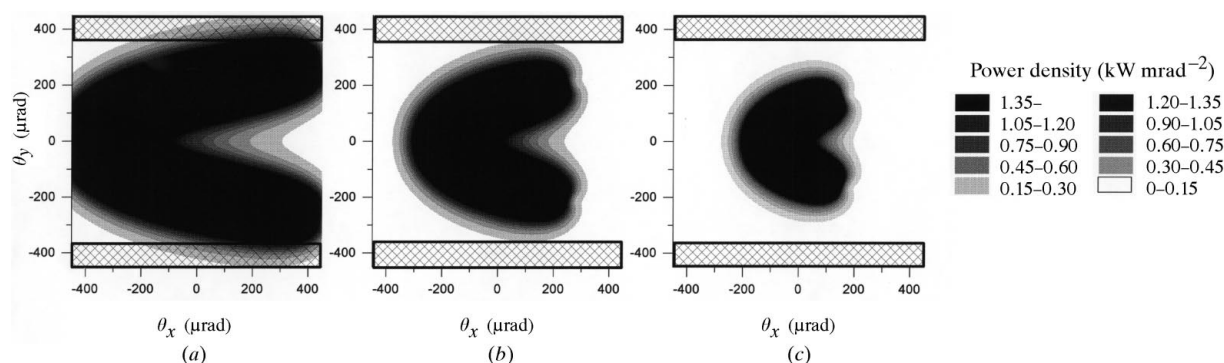
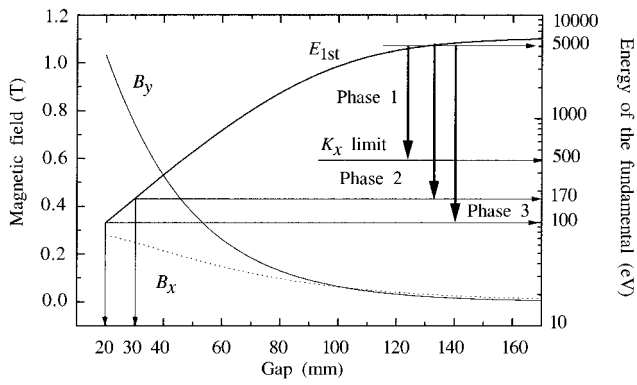


Figure 3

Spatial distributions of the power density from the figure-8 undulator for various values of the gap. Cross-hatched areas show the slot including an alignment error. (a) Gap = 31 mm,  $E_{1st} = 200 \text{ eV}$  ( $K_x = 4.44$ ,  $K_y = 6.25$ ). (b) Gap = 50 mm,  $E_{1st} = 500 \text{ eV}$  ( $K_x = 3.29$ ,  $K_y = 3.35$ ). (c) Gap = 66 mm,  $E_{1st} = 1000 \text{ eV}$  ( $K_x = 2.45$ ,  $K_y = 3.97$ ).



**Figure 4**  
Gap dependence of the vertical and horizontal magnetic fields and the energy of the fundamental.

effective  $K_x$  value at which the on-axis power density is efficiently suppressed keeping the intensity of the fundamental as high as possible. It has been found that the effective  $K_x$  of the figure-8 undulator is between 2 and 3 (Tanaka, 1996). The maximum  $K_x$  of the figure-8 undulator for BL27SU is 4.88, a little too high compared with the effective  $K_x$ . This is because the vertical and horizontal fields cannot be tuned independently. In order to make the figure-8 undulator more useful, it may be necessary to adopt a structure which can adjust the horizontal and vertical fields independently.

#### References

- Kitamura, H. (1995). *Rev. Sci. Instrum.* **66**, 2007–2010.  
 Tanaka, T. (1996). *Report of the SPring-8 International Workshop on 30 m-Long Straight Sections*. SPring-8, Kamigori-cho, Hyogo 678-12, Japan.  
 Tanaka, T. & Kitamura, H. (1995). *Nucl. Instrum. Methods*, **A364**, 368–373.